

High Gain Substrate Integrated Waveguide Fed Yagi-Uda Antenna Array on Silicon Substrate for Multiband Applications

Arnab Chakraborty* and Shweta Srivastava

Abstract—This paper proposes a Yagi-Uda antenna array realized on a Silicon substrate and supported by a substrate integrated waveguide for multi-band operation in the K and K_a bands. The structure of the dipole and the first director of the Yagi-Uda antenna were modified and tuned for multi-band response, making it completely novel in comparison to the existing Yagi-Uda structures supporting multi-band operation. As the feed, a substrate integrated waveguide was designed to assist with multi-band operation and to overcome the challenges presented by the Silicon substrate. An array is implemented to improve the gain. The antenna array's prototype was constructed and tested to back up the claims. The proposed array operates at frequencies of 23.7, 26.3, 27.5–28.3, and 29.4 GHz. The array exhibits good end-fire radiation patterns for the resonant frequencies, with a peak gain of 19.65 dBi and an efficiency of 89.8% at 23.7 GHz. This is the first report of an antenna fed by a substrate integrated waveguide and realized on Silicon with a high gain and applications in the K and K_a bands.

1. INTRODUCTION

Due to the ease of fabrication and high gain, the Yagi-Uda antenna is a salient element in present-day communication systems. There have been a large number of studies on the properties and design methodologies of Yagi-Uda antennas with multiple directors [1–4], where printed antennas are mostly used with features like ease of integration and low cost. But with complicated feeding structures, the implementation becomes difficult. An accepted solution is to implement a coplanar waveguide (CPW) or a substrate integrated waveguide (SIW) to feed the antenna. CPW or SIW feeding is also very helpful while designing an antenna on a Silicon (Si) substrate. Also, research regarding the implementation of Yagi-Uda as a multi-band antenna has not been done extensively. Multifunctional antennas, especially multimode and multi-band antennas, have become very popular with the advancement of wireless technology because of their dependability and adaptability. With the feature of frequency selectivity, multi-band antennas are quite useful for the use in several modern communication systems. In [5] & [6], quasi-Yagi type antennas were implemented with branch-like structures for multi-band operations. In [7], slot lines were inserted inside the driver, and branch line directors designed for different frequencies were used to implement multi-band operation. In [8], another quasi-Yagi antenna was presented for multi-band operations using a reformed bow-tie antenna. However, in all the above-mentioned papers gain is not adequate. In this research article, a Yagi-Uda antenna array with a new configuration fed by a SIW has been proposed for multi-band operation and high gain.

Realizing an antenna on a Si substrate is helpful for future on-chip implementation and integration. However, designing an antenna for high frequencies on a Si substrate has challenges. When operating at high frequencies, the high relative permittivity ($\epsilon_r = 11.9$) of Si causes surface waves that lessen the radiation performance of the antenna. A SIW feed for the antenna is a good solution as it reduces the surface waves. Another advantage of using SIW in the proposed design is SIWs have excellent immunity

Received 7 October 2021, Accepted 2 December 2021, Scheduled 19 December 2021

* Corresponding author: Arnab Chakraborty (17402005@mail.jiit.ac.in).

The authors are with the Jaypee Institute of Information Technology, Noida, India.

to electromagnetic interference, which leaves the scope for the proposed antenna array to be integrated with on-chip circuits as electromagnetic interference is a major concern while integrating antennas and circuits on-chip. Also feeding the antenna with a SIW is very helpful in obtaining multi-band operations as SIWs have a very broad operating frequency range. A lot of work has been done on antennas on Si substrate, but not for K and K_a bands. In [9] & [10], antennas realized on Si substrate were fed using SIW. A W-band end-fire directional antenna for 89.5-101 GHz realized on a single Si substrate was presented in [9]. A Yagi antenna operating between 9.4 and 10.05 GHz with a non-planar director was presented in [10]. In [11], a high gain and high-efficiency 3D Yagi-like antenna on Si for 340 GHz backed by a SIW cavity was presented. In [12], an on-chip rectangular slot antenna etched in SIW for 340 GHz realized in Si was presented. This paper presents a SIW fed antenna realized on a Si substrate with high gain and applications in K and K_a bands for the first time.

K and K_a bands offer a wide variety of applications requiring high data-rate communication. Frequencies like 24, 26, and 28 GHz from K and K_a bands are future candidates for 5G communication systems, but limited investigation has been done on these frequencies to understand their applicability. In [13], losses occurring in 24 GHz band due to parameters like interference, uplink, downlink sensitivity, etc. were experimentally analyzed to support and justify spectrum allocation at 24 GHz. In [14], a detailed study on attenuation due to rain at 26 GHz band has been done, and the applicability of 26 GHz band even in areas with high rain fall has been suggested. In [15], the advantages and applicability of 28 GHz band for future 5G communication have been suggested and supported by experimental results. In the proposed work, 24, 26, and 28 GHz frequencies have been selected as targeted operating frequencies because of the above mentioned reasons. The following format is used to describe this work: design and results of the SIW, the Yagi-Uda antenna's design and performance for multi-band operations, design and results of the 2-element array, and finally the overall conclusion.

2. DESIGN AND RESULTS OF THE SINGLE ELEMENT SIW FED YAGI-UDA ANTENNA

2.1. Design and Results of the SIW

In Figure 1, the SIW feed for the antenna elements of the proposed array is shown. The SIW has a total of 16 vias. Here, the diameter of the vias is d , and p is the distance between the vias.

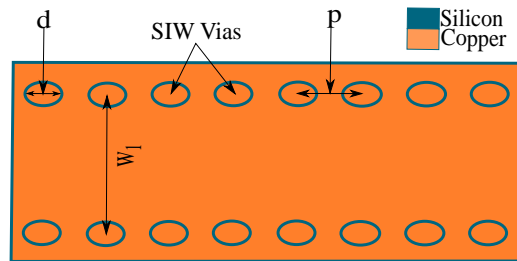


Figure 1. Layout of the SIW.

The reason for selecting the cut-off frequency (f_c) as 20 GHz of the proposed SIW has been discussed earlier in this paper. The design equations are given below,

$$f_c = \frac{c}{2\pi} \sqrt{\left(\frac{m\pi}{w}\right)^2 + \left(\frac{n\pi}{b}\right)^2} \quad (1)$$

where c is the speed of light; m and n are the mode numbers; and w and b represent the width and height of an equivalent rectangular waveguide (RWG) [16]. As SIW only supports TE_{10} mode, Equation (1) can be simplified into,

$$f_c = \frac{c}{2w} \quad (2)$$

Now, if an equivalent dielectric filled waveguide (DFW) has the same cut-off frequency, then the width of the DFW (w_d) can be obtained by,

$$w_d = \sqrt{\frac{w}{\epsilon_r}} \tag{3}$$

where ϵ_r is the dielectric constant of the DFW. With the value of w_d , the value of another important design parameter of SIW, w_1 , can be found by using [17],

$$w_1 = w_d + \frac{d^2}{0.95p} \tag{4}$$

where,

$$d < \frac{\lambda_g}{5} \tag{5}$$

$$p < 2d \tag{6}$$

The values of d and p can be found using Equation (5) and Equation (6), where λ_g is the guided wavelength and is defined by,

$$\lambda_g = \frac{2\pi}{\sqrt{\frac{\epsilon_r(2\pi f)^2}{c^2} - \left(\frac{\pi}{w}\right)^2}} \tag{7}$$

Here, f is the targeted operating frequency of SIW. The bandwidth of the SIW gets narrow and shifts to the higher frequency side as we increase d or p . So using Equations (5), (6), and (7), the values of d and p have been selected in such a manner that the proposed SIW covers all the targeted frequencies: 24, 26, and 28 GHz. The final values of the SIW design parameters are $w_1 = 7$ mm, $d = 1.5$ mm, and $p = 2.5$ mm. In Figure 2, the simulated (using ANSYS) insertion loss (S_{21}) and reflection coefficient (S_{11}) of the waveguide are shown. From the S_{11} plot, it is clear that the proposed SIW is working for the frequency range of 20–30 GHz.

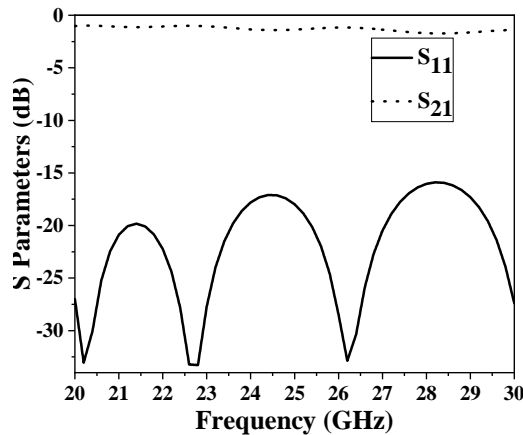


Figure 2. Simulated reflection coefficient and insertion loss of the proposed SIW.

2.2. Concept, Design and Results of the SIW Fed Single Element Multiband Yagi-Uda Antenna

A Yagi-Uda antenna in its traditional design adapted for a microstrip line appears similar to the layout depicted in Figure 3(a). The dipole driver and directors have the same width throughout their length which makes them work for a single frequency only. To solve this problem and make the antenna work for multi-band, branch line structures were used in [5] and [6], where different branch lines of the structure resonate for different frequencies making the antennas multi-bands. In [7], slot lines were inserted into the dipole driver, and a branch line director was designed to operate at different

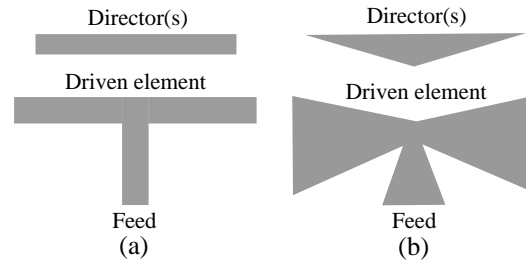


Figure 3. (a) Regular Yagi-Uda structure adapted into microstrip line. (b) Proposed modified structure for multiband output.

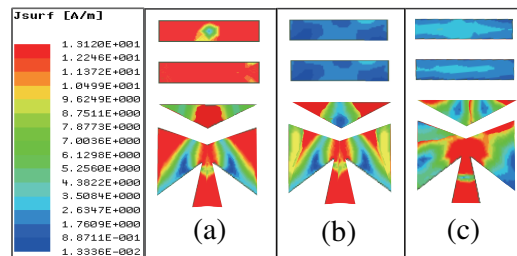


Figure 4. Current distributions of the proposed multiband Yagi-Uda antenna at (a) 23.7, (b) 26.3 and (c) 27.4 GHz.

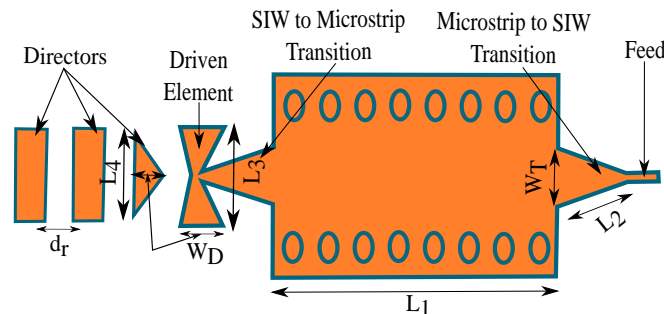


Figure 5. Layout of the single element with a microstrip to SIW feedline transition.

frequencies. Different regions of the dipole driver and the branch line director got active for different frequencies, and multi-band operation was achieved. [8] implements a reformed bow-tie driven element to achieve a wide bandwidth with the reflector working for lower frequencies and directors working for higher frequencies. In this paper, the multi-band output was achieved by giving a flared structure to the dipole driver along with a modified director (first of three) complementing the driver structure as shown in Figure 3(b). For three different frequencies, three different lengths and widths were selected, and then they were combined into the flared shape of the driven element and the first director. The first director was designed in such a way so that a uniform distance can be maintained throughout from the driven element. Different regions of the driven element and the director got activated for separate frequencies as depicted in Figure 4. Directors are good for increasing antenna performance, but directors designed for lower frequencies can also degrade antenna performance at higher frequencies by acting as reflectors. The other two directors were added later dedicated for the band with the highest gain.

Figure 5 depicts the proposed SIW fed Yagi-Uda antenna's layout. As discussed earlier in this paper, Si has been used as the substrate for the proposed antenna. The height of the substrate does not affect the properties of SIW, using that freedom, an available Si substrate with a height of 0.55 mm was used. The basic dimensions of the single element Yagi-Uda antenna have been taken from [18] and then optimized according to the design goals. As suggested in [18], the length of the driven element is

usually between 0.45 and $0.49\lambda_0$; the length of the directors is usually between 0.4 and $0.45\lambda_0$; and the distance between the elements is generally from 0.3 to $0.4\lambda_0$. Here, λ_0 is the wavelength in free space. The optimized values used in the proposed design satisfy the suggestions from [18]. To get a flat strip with near-zero thickness from a cylindrical dipole of diameter d_y , $w_y = 2d_y$ was considered, where w_y is the width of driver element and directors.

The proposed antenna's design specifications are as follows: $L_1 = 20.25$ mm, $L_2 = 4.78$ mm, $L_3 = 5.67$ mm, $L_4 = 4.8$ mm, $W_T = 2.8$ mm and $d_r = 1.75$ mm. The proposed antenna is fed using the SIW as discussed in the previous section. For practical implementation, a microstrip line to SIW transition for feeding the waveguide and a SIW to microstrip line transition for feeding the antenna have been used which is essential for the impedance matching. The width (W_T) and length (L_2) of the transition taper were calculated using [19]. L_3 and L_4 are the lengths of the driven element and directors, which are evidently the lengths calculated for 24 GHz as per our design considerations which limits the scope of analyzing the effect of change of length on resonating frequencies for the proposed design. As suggested in [20], width of the driven element of a dipole has a direct effect on its operating frequency. The width (W_D) is a combination of three different widths W_D , W_{26} , and W_{28} for frequencies 24, 26, and 28 GHz, respectively, where W_{26} depends on the ratio of $W_D : W_{28}$. Following [20], after combining the widths, parametric analysis was done to obtain the most suited values for the goal of the design. The effect of change of $W_D : W_{28}$ on reflection coefficient for resonating frequencies is shown in Figure 6. At $W_D : W_{28} = 1 : 0.45$, the best response was observed.

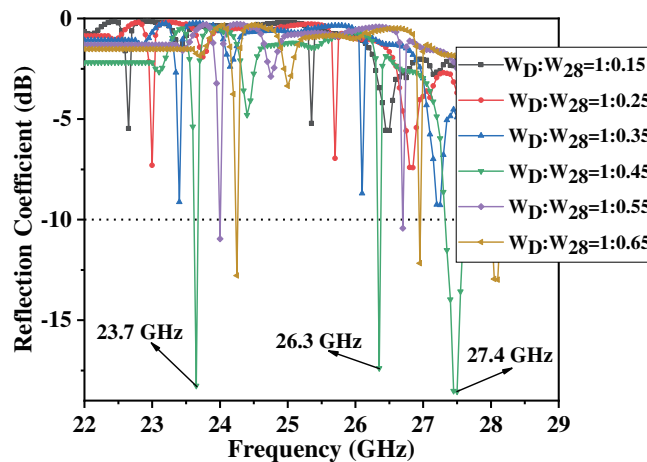


Figure 6. The effect of change of $W_D:W_{28}$ on reflection coefficient for the single element.

The proposed structure works for three frequencies, 23.7, 26.3, and 27.4 GHz. At 23.7 GHz, the highest peak gain of 10.2 dBi was observed after the initial simulation. The two additional directors were designed to work delicately for 23.7 GHz and added with the structure to increase the gain. The length and width of the additional directors are L_4 and W_D , respectively. The effect of the number of additional directors on peak gain is shown in Figure 7. As per Equation (8), reduced director spacing (d_r) can be achieved with a high dielectric constant like in Si, which helps in reducing the size of the overall structure [21]. Using that, the gap between the directors was optimized for maximum gain and compactness.

$$d_r = \frac{\lambda_0}{4} \times \frac{1}{\sqrt{\epsilon_r}} \tag{8}$$

After adding the two additional directors, simulated peak gain of 13.24 dBi at 23.7 GHz was achieved. The directors also improved the directivity of the antenna for 23.7 GHz. For all resonant frequencies, the antenna displays excellent end-fire radiation patterns. The simulated H -plane and E -plane radiation patterns of the proposed single element are shown in Figure 8.

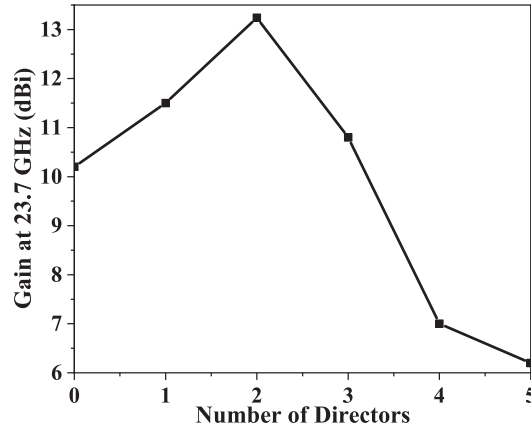


Figure 7. Variation of gain due to the added directors designed for 23.7 GHz.

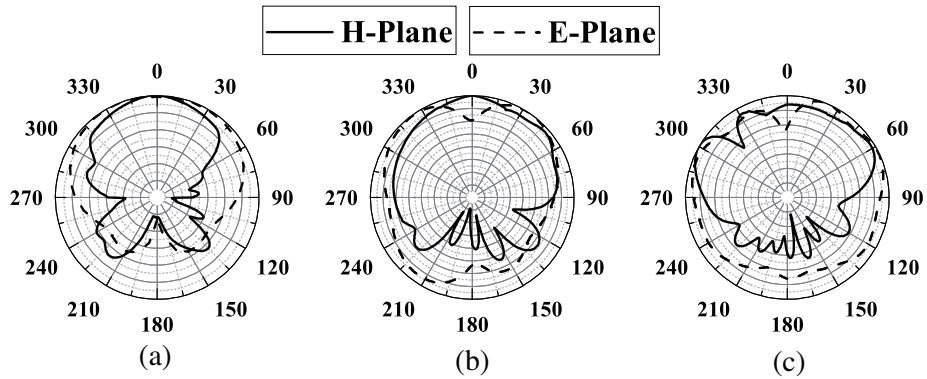


Figure 8. Simulated normalized radiation patterns of the single element at (a) 23.7, (b) 26.3 and (c) 27.4 GHz.

3. DESIGN AND RESULTS OF THE SIW FED YAGI-UDA ANTENNA ARRAY

In Figure 9(a), the layout of the proposed 2 element SIW fed Yagi-Uda antenna array is shown. Using the single element Yagi-Uda antenna discussed in the previous section, the proposed array is constructed. The edge to edge distances (D_1 & D_2) of the two antennas are kept the same, as 1 mm. Effect of increasing and decreasing D_1 & D_2 on the highest overall gain of the array is shown in Figure 9(b). As

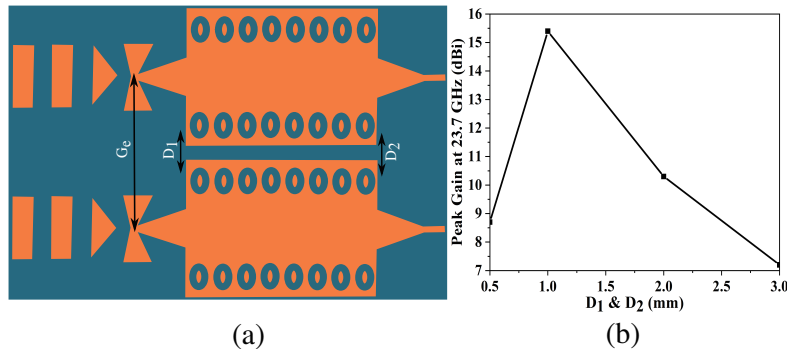


Figure 9. (a) Layout of the SIW fed 2 element Yagi-Uda antenna array. (b) Effect of D_1 and D_2 on the highest peak gain of the antenna array.

the distance between the elements increases, the gain of the array decreases due to decreased matching between the array elements. When the elements are placed 0.5 mm apart, the SIW feeds interfere with each other, and the gain is decreased. G_e is the center to center gap between elements.

To improve the gain, the center to center gap (G_e) between the two elements was further reduced. D_2 was increased with an angular increment of 5 degrees, while D_1 was kept fixed. Decreasing D_1 would have caused interference between the antenna elements, and increasing D_1 would have caused decreased matching between the array elements. The simulated effect of change of D_2 and G_e on the overall gain is shown in Table 1.

Table 1. Effect of change of D_2 and G_e on the highest peak gain of the array.

| Angular Rotation (Degrees) | D_2 (mm) | G_e (mm) | Highest Gain (dBi) |
|----------------------------|------------|------------|--------------------|
| 0 | 1 | 10.9 | 15.6 |
| 5 | 4.52 | 9.96 | 19.65 |
| 10 | 8.03 | 8.85 | 13.46 |
| 15 | 11.98 | 8.18 | 12.33 |

The modified array structure, shown in Figure 10, has almost the same resonating frequency bands as the single element with an additional one. Mutual coupling between the array elements accounts for the extra band. The four bands are 23.709 GHz, 26.372 GHz, Band-I containing frequencies 27.558 GHz to 28.372 GHz, and 29.444 GHz. The simulated and measured reflection coefficients of the modified array structure and the prototype are shown in Figure 11.

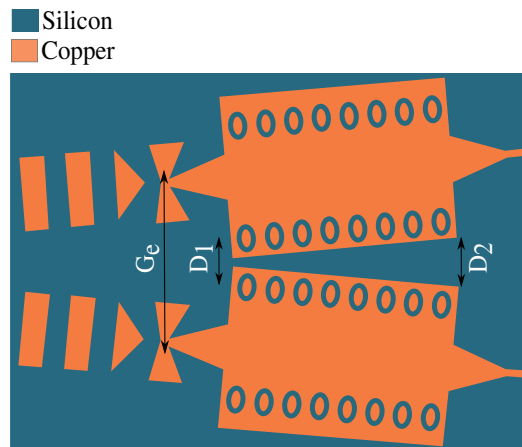


Figure 10. Layout of the modified array structure.

The gain of the array has improved for each of the resonating bands because of the better matching between the antenna elements due to the reduced G_e . The maximum peak gain of the modified array structure is 19.65 dBi at 23.7 GHz, which is a significant improvement over the single element and the basic array structure. Figure 12 depicts the simulated and measured variations of gain with frequency of the modified array. Simulated and measured radiation patterns are shown in Figure 13. 23.709 GHz has the highest gain, 19.65 dBi, directivity of 11.12 dBi, and 89.8% radiation efficiency. At 26.372 GHz, the peak gain is 10.54 dBi, directivity 10.81 dBi, and the radiation efficiency 97.07%. At Band-I, the highest gain is 16.08 dBi (27.63 GHz), and the directivity is 10.48 dBi. At 29.4 GHz, the peak gain is 11.50 dBi, and the directivity is 9.59 dBi.

To validate the design concepts, a prototype of the modified array was built and tested. A standard Si wafer was used as a substrate. The resistivity of the Si wafer is less than 10–20 Ωcm , and the thickness is $525 \pm 20 \mu\text{m}$. The major problems of fabricating an antenna using a Si wafer are: the rigidness of Si

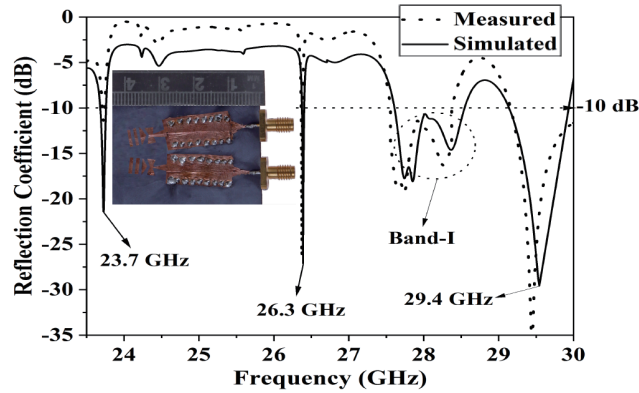


Figure 11. Simulated and measured reflection coefficient of the modified array and the fabricated structure.

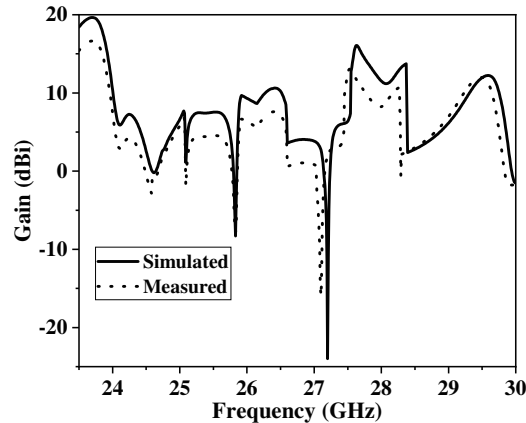


Figure 12. Simulated and measured variation of gain with frequency of the modified array.

wafer makes it impossible to print the circuit through any automated printing process and to drill holes in it as it shatters the wafer. To overcome these issues, a complete in-house fabrication was done. The fabricated prototype is shown in Figure 11. SMA 2.92 connectors were used to connect the prototype with the VNA for testing.

Despite all of the constraints encountered during fabrication, the the measured results of the prototype closely resemble the simulated output. The measured resonating frequencies are 23.72 GHz, 26.37 GHz, Band-I* containing frequencies from 27.55 to 28.37 GHz, and 29.45 GHz, which are remarkably similar to the simulated outcome. The measured peak gain at 23.72 GHz is 16.56 dBi, at 26.37 GHz is 7.1 dBi, and the highest measured gain for Band-I* is 12.95 dBi (27.55 GHz) and at 29.45 GHz is 11.91 dBi which is an improvement over the simulated gain. The normalized simulated and measured radiation patterns follow each other closely showing the effectiveness of the proposed array. In terms of directivities, the measured and simulated H -plane ($\phi = 0$) and E -plane ($\phi = 90$) patterns are close.

Very limited research has been done specifically in the area of the proposed work. In [5], branchline structures with microstrip to coplanar stripline feeding were proposed for multi-band operations. The operating frequency bands are 700–900 MHz with a gain of 4.4 dBi, 1575–1800 MHz with a gain of 1.1 dBi, and 2400 MHz with a gain of 0.3 dBi. In [6], branchline structures with a coplanar waveguide to coplanar stripline feeding were proposed for multi-band operations. The operating frequency bands are 1.85–2.0 GHz with directivity of 2.8 dBi, 2.25–3.05 GHz with directivity of 3.5 dBi, and 3.35–3.8 GHz with directivity of 5.1 dBi. The structural details of [7] have been discussed previously in this paper. It uses a microstrip feeding technique. The operating frequency bands are 1.9 GHz with a gain of 6.29 dBi,

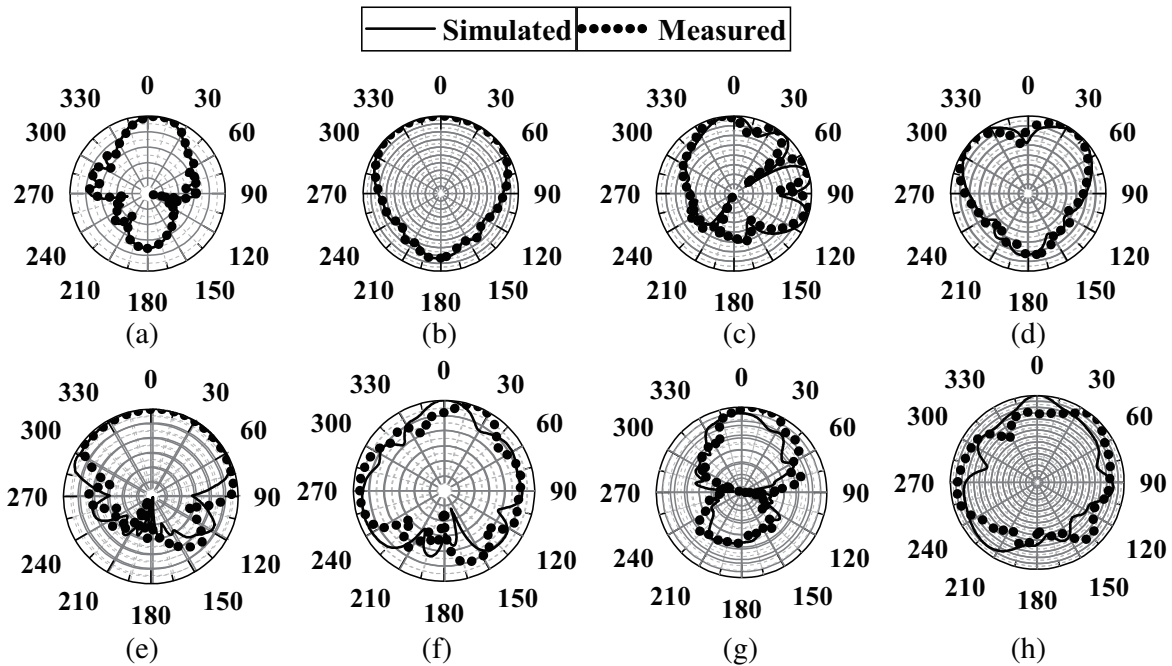


Figure 13. Simulated and measured radiation patterns of the modified array. 23.7 GHz: (a) *H*-plane, (b) *E*-plane. 26.3 GHz: (c) *H*-plane, (d) *E*-plane. 27.63 GHz: (e) *H*-plane, (f) *E*-plane. 29.4 GHz: (g) *H*-plane, (h) *E*-plane.

2.5 GHz with a gain of 4.63 dBi, and 3.5 GHz with a gain of 6.77 dBi. In [8], a quasi-Yagi antenna with a modified bow-tie driver has been used to achieve a very wide band of operation, 1.4–3.4 GHz with a highest gain of 7.5 dBi. Compared with [5–8], the proposed Yagi-Uda antenna array reported in this paper features a new structural concept for multi-band operations and performs better in terms of gain, directivity, and efficiency. Also with the SIW feeding a wide range of frequencies are covered as operating bands.

In [9–12], SIW was used as the feed, and proposed antennas are realized on Si. The comparison with this paper in terms of the type of antenna, operating frequencies, and gain is shown in Table 2.

Table 2. Comparison with other antennas fed by SIW and realized on Si.

| Reference | Type of antenna | Frequency (GHz) | Gain (dBi) |
|-----------|-----------------------|--------------------------------|-------------------------------|
| [9] | Planar dipole | 89.5–101 | 06.03 |
| [10] | Yagi monopulse | 9–11 | 09.46 |
| [11] | Yagi-like 3D | 320–360 | 10.00 |
| [12] | Rectangular slot loop | 340 | 07.90 |
| This work | Flared Yagi-Uda | 23.7, 26.3, 27.5–28.3 and 29.4 | 19.65, 10.54, 16.08 and 11.50 |

4. CONCLUSION

In this paper, a 2 element multi-band Yagi-Uda antenna array fed by SIW and realized on a Si substrate for *K* and *K_a* band applications is proposed and studied. The flared structures of the driven element and the first director compliment each other and achieve multiple operating frequency bands. Feeding the element antennas of the array with SIW has helped with the wide range of operating frequencies and

reduction of surface waves caused by the Si substrate which results in good overall radiation performance of the array. The proposed array has four operating frequency bands, 23.7, 26.37, 27.5–28.37, and 29.4 GHz. Two directors were added and designed dedicatedly for the best performing frequency band 23.7 GHz in terms of gain. Additions of the directors increased the peak gain and directivity of the single element at 23.7 GHz. Further, an array was implemented, and the layout was adjusted in a way that the distance between the array elements was reduced by rotating them inwards which results in better matching between the elements and in return results in the high gain of the proposed array. For 23.7 GHz, the proposed array achieves a peak gain of 19.65 dBi (simulated) and 16.57 dBi (measured) with an efficiency of 89.8%. A prototype of the proposed array was fabricated on a single Si substrate with a thickness of 0.55 mm which makes it a candidate for future integration with on-chip components. The measured and simulated results agree well, demonstrating the effectiveness of the proposed array.

REFERENCES

1. Mushiake, Y., "A report on Japanese development of antennas: From the Yagi-Uda antenna to self-complementary antennas," *IEEE Antennas Propag. Mag.*, Vol. 46, No. 4, 47–60, 2004.
2. Arceo, D. and C. A. Balanis, "A compact Yagi-Uda antenna with enhanced bandwidth," *IEEE Antennas Wirel. Propag. Lett.*, Vol. 10, No. 1, 44–445, 2011.
3. Lim, S. and H. Ling, "Design of a planar, closely spaced Yagi antenna," *IEEE Antennas Propag. Soc. AP-S Int. Symp.*, Vol. 5, 5997–6000, 2007.
4. Kramer, O., T. Djerafi, and K. Wu, "Vertically multilayer-stacked yagi antenna with single and dual polarizations," *IEEE Trans. Antennas Propag.*, Vol. 58, No. 4, 102–1030, 2010.
5. Wu, S. J., C. H. Kang, K. H. Chen, and J. H. Tarng, "A multiband quasi-yagi type antenna," *IEEE Trans. Antennas Propag.*, Vol. 58, No. 2, 593–596, 2010.
6. Ding, Y., Y. C. Jiao, P. Fei, B. Li, and Q. T. Zhang, "Design of a multiband Quasi-Yagi-type antenna with CPW-to-CPS transition," *IEEE Antennas Wirel. Propag. Lett.*, Vol. 10, 1120–1123, 2011.
7. Cheong, P., K. Wu, W. W. Choi, and K. W. Tam, "Yagi-uda antenna for multiband radar applications," *IEEE Antennas Wirel. Propag. Lett.*, Vol. 13, 1065–1068, 2014.
8. Zhao, T., Y. Xiong, X. Yu, H. Chen, M. He, L. Ji, X. Zhang, X. Zhao, H. Yue, and F. Hu, "A broadband planar Quasi-Yagi antenna with a modified bow-tie driver for multi-band 3G/4G applications," *Progress In Electromagnetics Research C*, Vol. 71, 59–67, 2017.
9. Deng, Y., F. Zhu, B. Li, J. Zhang, and Z. Zhou, "Design of a compact W-band planar dipole antenna on a single silicon substrate," *2019 Int. Conf. Microw. Millim. Wave Technol. ICMMT 2019 — Proc.*, Vol. 128, 2019–2021, 2019.
10. Zou, X., C. M. Tong, J. S. Bao, and W. J. Pang, "SIW-fed Yagi antenna and its application on monopulse antenna," *IEEE Antennas Wirel. Propag. Lett.*, Vol. 13, 1035–1038, 2014.
11. Deng, X. D., Y. Li, C. Liu, W. Wu, and Y. Z. Xiong, "340 GHz on-chip 3-D antenna with 10 dBi gain and 80% radiation efficiency," *IEEE Trans. Terahertz Sci. Technol.*, Vol. 5, No. 4, 619–627, 2015.
12. Deng, X. D., Y. Li, W. Wu, and Y. Z. Xiong, "340-GHz SIW cavity-backed magnetic rectangular slot loop antennas and arrays in silicon technology," *IEEE Trans. Antennas Propag.*, Vol. 63, No. 12, 5272–5279, 2015.
13. Xu, Y. and Q. Zhaojun, "Research on interference test of 24 GHz millimeter wave radar to 5G equipment," *J. Phys. Conf. Ser.*, Vol. 1584, No. 1, 2020.
14. Shayea, I., T. Abd Rahman, M. Hadri Azmi, and M. R. Islam, "Real measurement study for rain rate and rain attenuation conducted over 26 GHz microwave 5G link system in Malaysia," *IEEE Access*, Vol. 6, 19044–19064, 2018.
15. Rappaport, T. S., S. Sun, R. Mayzus, H. Zhao, Y. Azar, K. Wang, G. N. Wong, J. K. Schulz, M. Samimi, and F. Gutierrez, "Millimeter wave mobile communications for 5G cellular: It will work!," *IEEE Access*, Vol. 1, 335–349, 2013.

16. Djera, T., A. Doghri, and K. Wu, *Handbook of Antenna Technologies*, Springer Science+Business Media, Singapore, 2016.
17. Wu, K., D. Deslandes, and Y. Cassivi, "The substrate integrated circuits — A new concept for high-frequency electronics and optoelectronics," *6th Int. Conf. Telecommun. Mod. Satell. Cable Broadcast. Serv. TELSIKS 2003 — Proc.*, Vol. 1, 2003.
18. Balanis, C. A., *Antenna Theory: Analysis and Design*, John Wiley & Sons, Inc, Hoboken, New Jersey, 2005.
19. Deslandes, D., "Design equations for tapered microstrip-to-Substrate Integrated Waveguide transitions," *IEEE MTT-S Int. Microw. Symp. Dig.*, Vol. 128, 704–707, 2010.
20. Jamaluddin, M. H., M. K. A. Rahim, M. Z. A. A. Aziz, and A. Asrokin, "Microstrip dipole antenna analysis with different width and length at 2.4 GHz," *2005 Asia-Pacific Conf. Appl. Electromagn. APACE 2005 — Proc.*, Vol. 2005, 41–44, 2005.
21. Dadgarpour, A., B. Zarghooni, B. S. Virdee, and T. A. Denidni, "High-gain end-fire bow-tie antenna using artificial dielectric layers," *IET Microwaves, Antennas Propag.*, Vol. 9, No. 12, 1254–1259, 2015.